THE EVOLUTION OF THE RELATIVE GAIN ARRAY MATRIX: THE MULTIVARIABLE STRUCTURE FUNCTION

Luis A. Amézquita-Brooks
CIIIA-FIME
UANL
México
luis.amezquita@uanl.mx

Carlos E. Ugalde-Loo
Institute of Energy
Cardiff University
Wales, UK
Ugalde-LooC@cardiff.ac.uk

Eduardo Licéaga-Castro
CIIIA-FIME
UANL
México
e.liceaga.c@gmail.com

Jesús Licéaga-Castro
Depto. de Electrónica
UAM-Azcapotzalco
México
ucastro21@hotmail.com

Abstract

Typically, the performance of a control design task is specified in terms of an output response to a given input. This is also the case for multivariable plants, where for clarity of performance specification and design it remains desirable to consider the inputs and outputs in pairs. Regardless of the structure and internal coupling of the plant, it is convenient to establish if decentralized control is capable of meeting design specifications: the control structure will be easy to implement, economic (less programming burden upon implementation), and may provide physical insight. In line with this, the analysis and design of decentralized controllers using the relative gain array (RGA) and the multivariable structure function (MSF) are presented for the general multivariable case. It is shown that the RGA matrix can be expressed in terms of the MSF. Theoretical results are drawn for a general $n{\times}n$ plant, with an example from electrical power systems included to illustrate key concepts.

Key words

Decentralized control, individual channel analysis and design, multivariable control, multivariable structure function, relative gain array.

1 The Relative Gain Array Matrix

The relative gain array (RGA) matrix, proposed by [Bristol, 1966], is defined as:

$$\mathbf{\Lambda}\big(\mathbf{G}(s)\big) = \mathbf{G}(s) \times \big(\mathbf{G}(s)^{-1}\big)^T, \qquad (1)$$

where $\times$ denotes an element-by-element multiplication and $\mathbf{G}(s)$ is an $n{\times}n$ square transfer matrix:

$$\mathbf{G}(s) = \begin{bmatrix} g_{11}(s) & g_{12}(s) & \dots & g_{1n}(s) \\ g_{21}(s) & g_{22}(s) & \dots & g_{2n}(s) \\ \vdots & \vdots & \ddots & \vdots \\ g_{n1}(s) & g_{n2}(s) & \dots & g_{nn}(s) \end{bmatrix}. \qquad (2)$$

Historically, the use of the RGA matrix has been focused on decentralized (diagonal) control. In particular, the following rules regarding the pairing of input-output control channels are employed [Skogestad and Postlethwaite, 2005]:

i. An input-output paring such that the diagonal elements of the RGA matrix are close to one is preferable since this paring is related with a diagonal dominant plant.

ii. Avoid input-output parings which generate diagonal negative elements on the RGA matrix with $s = 0$. This condition is closely related to systems with lack of integrity; *i.e.*, a system which cannot maintain stability if one of the diagonal closed loops is open.

iii. High positive values in the diagonal elements of the RGA matrix indicate difficulty for designing diagonal controllers.

RGA has proved to be a valuable tool in the selection of input-output pairing for diagonal control design. In general RGA can be interpreted in the frequency domain, but it is commonly used to evaluate the coupling of input-output pairings at steady state [Bristol, 1966; Grosdidier, Morari and Holt, 1985]. However, it has been observed that rule i should be applied with $s = j\omega_{BW}$, where ω_{BW} is the crossover frequency of

the open loop system [Mc Avoy, Arkun, Chen, Robinson and Schnelle, 2003; Skogestad and Postlethwaite, 2005].

Even when the use of the RGA matrix is widely accepted, developments of the key ideas which are contained within the theoretical foundations of the RGA matrix have not been fully analyzed. The main idea around the RGA matrix is to assess the effect a controller of each output variable would have on a specific open loop variable. In fact, the ij-th element of matrix $\mathbf{G}(s)$ may be defined as follows:

$$\lambda_{ij} = \frac{g_{ij}(s)}{\hat{g}_{ij}(s)}, \tag{3}$$

where $\hat{g}_{ij}(s)$ is the resulting open loop response between the j-th input and the i-th output with all the remaining outputs set under the influence of a diagonal controller of appropriate dimensions.

It would seem logical to ask what would be the stability and robustness characteristics of such a controller. Some effort in this direction was presented in [Grosdidier, Morari and Holt, 1985; Chiu and Arkun, 1990; Skogestad and Postlethwaite, 2005], where the integrity of the control system in relation with the RGA matrix was investigated. However, the RGA matrix does not play any role in the design stage of the controller. Moreover, its use has been restricted to those systems which can be made diagonal dominant by the simple commutation of input-output parings.

In a completely independent fashion, a multivariable design framework called Individual Channel Analysis and Design (ICAD), which deals with the design of diagonal controllers for multivariable plants, was proposed in the early 90s [O'Reilly and Leithead, 1991]. Although not widespread, this framework proved useful in solving difficult control problems associated to non-diagonally dominant, unstable, non-minimum phase and non-square plants [Licéaga-Castro, Licéaga-Castro and Ugalde-Loo, 2005; Licéaga-Castro, Licéaga-Castro and Amézquita-Brooks, 2005; Licéaga-Castro, Ramírez-España and Licéaga-Castro, 2006; Licéaga-Castro, Licéaga-Castro, Ugalde-Loo and Navarro-López, 2008; Licéaga-Castro, Amézquita-Brooks and Licéaga-Castro, 2008; Ugalde-Loo, 2009].

ICAD allows the use of classical SISO robustness margins (phase and gain margin) for MIMO control systems. The key component of the ICAD framework is the *Multivariable Structure Function* (MSF) which illuminates several important issues of the open loop system. In particular, it allows

- elucidating the minimum phase conditions of the transmission zeros;
- measuring the cross-coupling between input-output pairs;
- using the Nyquist stability criterion, and all its associated robustness margins, for measuring the possibility of direct decoupling of the system.

It is clear that a close relationship between the MSF and the RGA matrix should exist since through both tools appropriate input-output parings can be defined. In the next sections this relation will be fully revealed and some common features will be analyzed. However, it should be noticed that the most important features of the MSF are not related with the analysis of the open loop system. As a matter of fact, the MSF plays a crucial part both in the controller design process and in the subsequent robustness assessment of the closed loop control system.

2 The Multivariable Structure Function

Consider an $n \times n$ system $\mathbf{G}(s)$ with a diagonal controller matrix $\mathbf{K}(s)$:

$$\begin{aligned}
\mathbf{Y}(s) &= \mathbf{G}(s)\mathbf{U}(s), \\
\mathbf{U}(s) &= \mathbf{K}(s)\mathbf{E}(s), \\
\mathbf{E}(s) &= \mathbf{R}(s) - \mathbf{Y}(s),
\end{aligned} \tag{4}$$

where $\mathbf{R}(s)$ is a reference vector. The output and input signal vectors are defined, respectively, as follows:

$$\begin{aligned}
\mathbf{Y}(s) &= \begin{bmatrix} y_1(s) \; y_2(s) \; \ldots \; y_n(s) \end{bmatrix}^T, \\
\mathbf{U}(s) &= \begin{bmatrix} u_1(s) \; u_2(s) \; \ldots \; u_n(s) \end{bmatrix}^T.
\end{aligned}$$

The closed loop dynamics of (4) are given by:

$$\begin{aligned}
\mathbf{Y}(s) &= \mathbf{G}(s)\mathbf{K}(s)\big(\mathbf{I} + \mathbf{G}(s)\mathbf{K}(s)\big)^{-1}\mathbf{R}(s) \\
&= \mathbf{H}(s)\mathbf{R}(s).
\end{aligned} \tag{5}$$

The individual channel concept is set up to investigate the cross-coupling of a particular group of input-output variables against the remaining variables. That is, system $\mathbf{G}(s)$ may be partitioned as

$$\mathbf{G}(s) = \left[\begin{array}{c|c} \mathbf{G}_{11}(s) & \mathbf{G}_{12}(s) \\ \hline \mathbf{G}_{21}(s) & \mathbf{G}_{22}(s) \end{array} \right], \tag{6}$$

with

$$\begin{aligned}
\mathbf{Y}(s) &= \begin{bmatrix} \mathbf{Y}_1(s) \\ \mathbf{Y}_2(s) \end{bmatrix}, \quad \mathbf{K}(s) = \left[\begin{array}{c|c} \mathbf{K}_{11}(s) & \mathbf{0} \\ \hline \mathbf{0} & \mathbf{K}_{22}(s) \end{array} \right], \\
\mathbf{R}(s) &= \begin{bmatrix} \mathbf{R}_1(s) \\ \mathbf{R}_2(s) \end{bmatrix}, \quad \mathbf{E}(s) = \begin{bmatrix} \mathbf{E}_1(s) \\ \mathbf{E}_2(s) \end{bmatrix}.
\end{aligned} \tag{7}$$

A block diagram depicting the system described by (6) and (7) is shown in Figure 1.

For the following procedure the Laplace operator is dropped for convenience. According to Figure 1,

$$\mathbf{Y}_1 = \mathbf{G}_{11}\mathbf{U}_1 + \mathbf{G}_{12}\mathbf{U}_2.$$

Notice that $\mathbf{U}_2(s)$ may also be written as

$$\mathbf{U}_2 = \mathbf{X}_2\boldsymbol{\delta}_2,$$

where

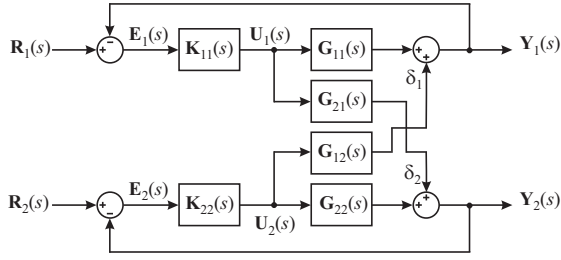$$\boldsymbol{\delta}_2 = \mathbf{G}_{21}\mathbf{U}_1.$$

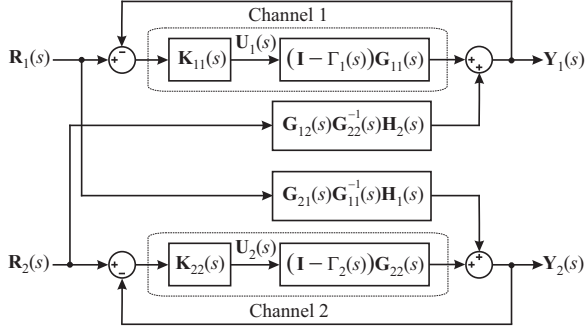Figure 1. Block diagram representation of a partitioned multivariable control system with a diagonal controller.

Figure 2. Equivalent control system using individual channel representation.

$\mathbf{X}_2(s)$ can be easily obtained noting that

$$\mathbf{U}_2 = \mathbf{K}_{22}\mathbf{E}_2,$$
$$\mathbf{E}_2 = \mathbf{R}_2 - (\mathbf{G}_{22}\mathbf{U}_2 + \boldsymbol{\delta}_2).$$

By using the superposition theorem and considering $\mathbf{R}_2(s) = \mathbf{0}$, then

$$\mathbf{U}_2 = -\mathbf{K}_{22}(\boldsymbol{\delta}_2 + \mathbf{G}_{22}\mathbf{U}_2).$$

A rearrangement of the previous expression by using the "push through" rule [Helton, Stankus and Wavrik, 1998] yields

$$\mathbf{U}_2 = -\mathbf{K}_{22}(\mathbf{I} + \mathbf{G}_{22}\mathbf{K}_{22})^{-1}\boldsymbol{\delta}_2.$$

Considering this, $\mathbf{Y}_1(s)$ can be rewritten as

$$\mathbf{Y}_{1a} = \mathbf{G}_{11}\mathbf{U}_1 - \mathbf{G}_{12}\mathbf{K}_{22}(\mathbf{I} + \mathbf{G}_{22}\mathbf{K}_{22})^{-1}\mathbf{G}_{21}\mathbf{U}_1,$$

where $\mathbf{Y}_{1a}(s)$ was introduced to remark that $\mathbf{R}_2(s) = \mathbf{0}$. Since the closed loop of the diagonal open loop transfer matrix $\mathbf{G}_{22}(s)\mathbf{K}_{22}(s)$ can be expressed as

$$\mathbf{H}_2 = \mathbf{G}_{22}\mathbf{K}_{22}(\mathbf{I} + \mathbf{G}_{22}\mathbf{K}_{22})^{-1},$$

it is clear then that

$$\mathbf{Y}_{1a} = \left(\mathbf{I} - \mathbf{G}_{12}\mathbf{G}_{22}^{-1}\mathbf{H}_2\mathbf{G}_{21}\mathbf{G}_{11}^{-1}\right)\mathbf{G}_{11}\mathbf{K}_{11}\mathbf{E}_1,$$

or, more compactly,

$$\mathbf{Y}_{1a} = (\mathbf{I} - \boldsymbol{\Gamma}_1)\mathbf{G}_{11}\mathbf{K}_{11}\mathbf{E}_1 = \mathbf{C}_1\mathbf{E}_1, \qquad (8)$$

where

$$\mathbf{C}_1(s) = (\mathbf{I} - \boldsymbol{\Gamma}_1(s))\mathbf{G}_{11}(s)\mathbf{K}_{11}(s) \qquad (9)$$

represents Individual Channel 1 and models the open loop response of the output variables $\mathbf{Y}_1(s)$ under the fact that variables $\mathbf{Y}_2(s)$ operate in closed loop with controller $\mathbf{K}_2(s)$. The key element of the preceding analysis is the MSF $\boldsymbol{\Gamma}_1(s)$, defined as

$$\boldsymbol{\Gamma}_1 = \mathbf{G}_{12}(s)\mathbf{G}_{22}(s)^{-1}\mathbf{H}_2(s)\mathbf{G}_{21}(s)\mathbf{G}_{11}(s)^{-1}, \quad (10)$$

which will be shown in the following Section to be closely related to the RGA matrix.

In order to elucidate the effect of $\mathbf{R}_2(s)$ over $\mathbf{Y}_1(s)$, consider that the control loop over $\mathbf{E}_1(s)$ is open. This implies that

$$\mathbf{E}_2(s) = \mathbf{R}_2(s) - \mathbf{Y}_2(s).$$

Thus,

$$\mathbf{U}_2(s) = \mathbf{K}_{22}(s)\left(\mathbf{I} + \mathbf{G}_{22}(s)\mathbf{K}_{22}(s)\right)^{-1}\mathbf{R}_2(s),$$
$$= \mathbf{G}_{22}(s)^{-1}\mathbf{H}_2(s)\mathbf{R}_2(s).$$

This rearrangement is represented in the block diagram of Figure 2, where the corresponding equations for Individual Channel 2 can be derived by simple symmetry. In particular:

$$\boldsymbol{\Gamma}_2(s) = \mathbf{G}_{21}(s)\mathbf{G}_{11}(s)^{-1}\mathbf{H}_1(s)\mathbf{G}_{12}(s)\mathbf{G}_{22}(s)^{-1},$$
$$\mathbf{H}_1(s) = \mathbf{G}_{11}(s)\mathbf{K}_{11}(s)\left(\mathbf{I} + \mathbf{G}_{11}(s)\mathbf{K}_{11}(s)\right)^{-1}.$$

The importance of MSFs $\boldsymbol{\Gamma}_i(s)$ becomes clear when, for instance, $\boldsymbol{\Gamma}_1(s) = \mathbf{0}$. This situation implies that the open loop response of variables $\mathbf{Y}_1(s)$ are equal to $\mathbf{G}_{11}(s)\mathbf{K}_{11}(s)\mathbf{E}_1(s)$ if $\mathbf{R}_2(s) = \mathbf{0}$. That is, subsystem $\mathbf{G}_{11}(s)$ is not coupled with subsystem $\mathbf{G}_{22}(s)$ through controller $\mathbf{K}_{11}(s)$. This indicates that it is possible to design $\mathbf{K}_{11}(s)$ on the basis of $\mathbf{G}_{11}(s)$ only.

The assumption that $\mathbf{R}_2(s) = \mathbf{0}$ can be lifted with no real consequences provided that the closed loop sensitivity of $\mathbf{G}_{11}(s)\mathbf{K}_{11}(s)$ is able to reject the perturbation $\mathbf{G}_{12}(s)\mathbf{G}_{22}(s)^{-1}\mathbf{H}_2(s)\mathbf{R}_2(s)$. Even if that is not the case, the stability of the system is not compromised given that $\mathbf{H}_2(s)$ is stable. Therefore, MSFs $\boldsymbol{\Gamma}_i(s)$ effectively measure the coupling of the system, with a high value of $\|\boldsymbol{\Gamma}_i(j\omega_0)\|$ (using an appropriate norm) indicating a high coupling between variables $\mathbf{Y}_1(s)$ and $\mathbf{Y}_2(s)$ at frequency ω_0. Such a notion of coupling allows the introduction of a clear measurement of cross-coupling.

A full treatment of the ICAD framework is out of the scope of this article; however, it will be shown that the MSF is an extension of the RGA matrix.

3 Relation between the RGA matrix and the MSF

The contexts in which the RGA matrix and the MSF were derived are different: while the RGA matrix was obtained for open loop plant analysis [Bristol, 1966], the MSF was established as a means to measure

the robustness of the closed loop system in the context of control design [O'Reilly and Leithead, 1991]. Nonetheless, equivalent assumptions may be considered for both.

For instance, when calculating λ_{ij}, the ij-th element of the RGA matrix $\mathbf{\Lambda}\big(\mathbf{G}(s)\big)$ defined in (3), it is assumed that all outputs, excluding y_i, are perfectly controlled using all inputs, excluding u_j. In this context the open loop response of the free input-output variables y_i and u_j is denoted as $\hat{g}_{ij}(s)$. Such perfect control assumption can be also made within the ICAD framework. In this case, it is assumed that variables $\mathbf{Y}_2(s)$ are perfectly controlled via inputs $\mathbf{U}_2(s)$, which is equivalent to assuming $\mathbf{Y}_2(s) = \mathbf{R}_2(s)$. In this situation the input-output response between references $\mathbf{R}_2(s)$ and outputs $\mathbf{Y}_2(s)$ is given by $\mathbf{Y}_2(s) = \mathbf{H}_2(s)\mathbf{R}_2(s)$, since the variables $\mathbf{Y}_1(s)$ and inputs $\mathbf{U}_1(s)$ are operating in open loop (see Figure 1). Therefore, $\mathbf{Y}_2(s) = \mathbf{R}_2(s)$ is equivalent to $\mathbf{H}_2(s) = \mathbf{I}$.

Nevertheless, whilst the MSF and the individual channel definitions allow for multivariable individual channels, or multi-channels [Leithead and O'Reilly, 1992], the RGA matrix elements λ_{ij} consider only scalar "free" input-output variables. Employing such a consideration with scalar input u_1 and output y_1, for instance, is equivalent to assuming that $\mathbf{Y}_1(s) = y_1(s)$ and $\mathbf{U}_1(s) = u_1(s)$. Under these conditions and since $\mathbf{U}_1(s) = \mathbf{K}_{11}(s)\mathbf{E}_1(s)$, it is easy to show from (8) that

$$y_1(s) = \big(1 - \gamma_1(s)\big)g_{11}(s)u_1(s),$$

where

$$\gamma_1(s) = \mathbf{G}_{12}(s)\mathbf{G}_{22}(s)^{-1}\mathbf{G}_{21}(s)g_{11}(s)^{-1}$$

is the scalar MSF which relates Individual Channel 1 and the multi-channel formed by all the remaining outputs. The relationship between λ_{11} and $\gamma_1(s)$ is finally revealed by noting that

$$\hat{g}_{11}(s) = \big(1 - \gamma_1(s)\big)g_{11}(s).$$

Thus,

$$\lambda_{11} = \frac{g_{11}(s)}{\hat{g}_{11}(s)} = \frac{1}{\big(1 - \gamma_1(s)\big)}. \tag{11}$$

The previous analysis may be generalized for the remaining elements of the RGA matrix by simple symmetry. In general, the ij-th element of the RGA matrix may be written as

$$\lambda_{ij} = \frac{1}{\big(1 - \gamma_{ij}(s)\big)}. \tag{12}$$

where $\gamma_{ij}(s)$ is the MSF which relates the i-th output with the j-th input assuming that all remaining outputs are controlled perfectly with the remaining inputs. MSF $\gamma_{ij}(s)$ can be obtained by rearranging the columns (or rows) of transfer matrix $\mathbf{G}(s)$ into $\hat{\mathbf{G}}(s)$ so

that the i-th output and the j-th input of $\mathbf{G}(s)$ become the first output and the first input of $\hat{\mathbf{G}}(s)$. This way,

$$\gamma_{ij}(s) = \hat{\mathbf{G}}_{12}(s)\hat{\mathbf{G}}_{22}(s)^{-1}\hat{\mathbf{G}}_{21}(s)\hat{g}_{11}(s)^{-1},$$

which effectively consists of rearranging the inputs and output pairs of a diagonal controller.

For instance, consider a simple 2×2 control system; i.e., $\mathbf{G}_{ij}(s) = g_{ij}(s)$, with $i, j = 1, 2$. In this case,

$$\gamma_{11}(s) = \frac{g_{12}(s)g_{21}(s)}{g_{11}(s)g_{22}(s)}.$$

It is known that for a 2×2 system [Skogestad and Postlethwaite, 2005],

$$\lambda_{11} = \frac{1}{\left(1 - \dfrac{g_{12}(s)g_{21}(s)}{g_{11}(s)g_{22}(s)}\right)}. \tag{13}$$

For systems of higher order [Grosdidier, Morari and Holt, 1985; Skogestad and Postlethwaite, 2005],

$$\lambda_{ii} = \frac{g_{ii}(s)\det \mathbf{G}^{ii}}{\det \mathbf{G}(s)}. \tag{14}$$

where $\mathbf{G}^{ii}$ is the minor of the ii-th element of $\mathbf{G}(s)$. Therefore, it follows from (12) and (14) that

$$\gamma_{ii}(s) = \frac{\lambda_{ii} - 1}{\lambda_{ii}} = 1 - \frac{\det \mathbf{G}(s)}{g_{ii}(s)\det \mathbf{G}^{ii}}. \tag{15}$$

The off-diagonal elements of the RGA matrix $\mathbf{\Lambda}\big(\mathbf{G}(s)\big)$ can be related with the MSF by swapping the appropriate rows (or columns) in $\mathbf{G}(s)$.

The previous result sheds some light regarding the nature of the MSF. The individual channels considering the perfect control condition and a scalar output for $y_1(s)$ may be written as

$$c_i(s) = k_{ii}(s)g_{ii}(s)\big(1 - \gamma_i(s)\big).$$

Then, considering (15) and $\mathbf{H}_i(s) = \mathbf{I}$ yields:

$$c_i(s) = k_{ii}(s) \cdot \frac{\det \mathbf{G}(s)}{\det \mathbf{G}^{ii}}. \tag{16}$$

Equation (16) reveals the relationship between the MSF and the RGA matrix within the ICAD context. However, it is important to emphasize that whereas the RGA matrix has only been used to define input-output pairs selection as a previous step to diagonal control design, the MSF has been successfully applied directly in the control design procedure.

4 Differences between the RGA and the MSF

The main differences between the RGA matrix and the MSF are summarized as follows:

- The inclusion of the controller effects in the MSF allows its use as a measure of closed loop robustness.
- The RGA and the MSF have an interpretation in the frequency domain. However, the MSF analysis (magnitude and phase) is crucial to determine the existence of stabilizing controllers and their requirements [O'Reilly and Leithead, 1991].
- The MSF is not necessarily a scalar function. This allows using the MSF to measure the cross-coupling between arbitrary groups of output-input pairings. This is of great significance in processes where it is not possible to find decoupled scalar input-output pairs, but where decoupled groups of such pairings exist. For instance in airplanes the variables relating the longitudinal and horizontal dynamics are both highly coupled systems which, nonetheless are considered as decoupled among them [Cook, 2012].

5 Illustrative Example

In order to illustrate the results presented in Section 3 and to address the points from Section 4, consider the system described by Figure 3. It corresponds to a synchronous generator feeding into a large system (represented by an infinite bus) via a tie-line system including a shunt compensator in the form of a Static VAr Compensator (SVC). The main application of an SVC is to provide dynamic reactive power support to enable effective voltage regulation and to enhance transient stability [Aree and Acha, 1999]. However, if a damping control loop is included, the device is also capable to provide damping for electromechanical oscillations [Mithulananthan, Canizares, Reeve and Rogers, 2003]. Figure 4 shows a block diagram of the system.

The synchronous machine – SVC system can be represented as the 3×3 system shown in Figure 4 [Ugalde-Loo, Acha and Licéaga-Castro, 2010]. The transfer matrix representation of such a system has the form

$$
\begin{bmatrix} \Delta\omega(s) \\ \Delta e_t(s) \\ \Delta V_{svc}(s) \end{bmatrix} = \begin{bmatrix} g_{11}(s) & g_{12}(s) & g_{13}(s) \\ g_{21}(s) & g_{22}(s) & g_{23}(s) \\ g_{31}(s) & g_{32}(s) & g_{33}(s) \end{bmatrix} \begin{bmatrix} \Delta P_m(s) \\ \Delta E_{fd}(s) \\ \Delta\alpha(s) \end{bmatrix}
\tag{17}
$$

or, more compactly,

$$
\mathbf{Y}_{svc}(s) = \mathbf{G}_{svc}(s)\mathbf{U}_{svc}(s),
\tag{18}
$$

where $\mathbf{G}_{svc}(s)$ is the transfer matrix. The individual elements of $\mathbf{G}_{svc}(s)$ can be explicitly found in [Ugalde-Loo, Acha, Licéaga-Castro and Licéaga-Castro, 2008]. The synchronous machine parameters and operating condition are provided in [Ugalde-Loo, Acha and Licéaga-Castro, 2010].

System (17) is stable and has minimum phase transmission zeros. In addition, it has been shown in [Ugalde-Loo, Acha and Licéaga-Castro, 2010] that a stabilizing diagonal controller for this system is given by:
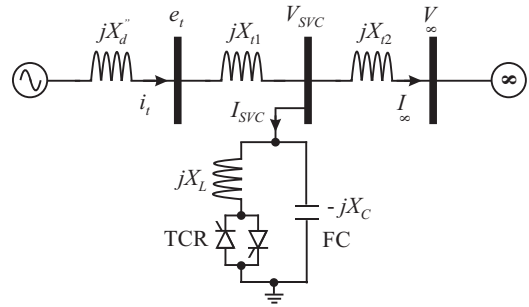

Figure 3. Synchronous generator – SVC system [Ugalde-Loo, Acha and Licéaga-Castro, 2010].
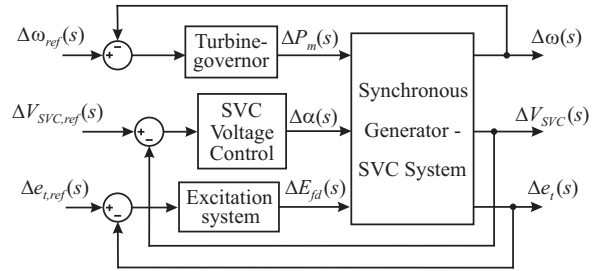

Figure 4. Block diagram of the synchronous generator – SVC system [Ugalde-Loo, Acha and Licéaga-Castro, 2010].

$$
\mathbf{K}_{SVC} = \mathrm{diag}\left[\frac{63(s+3.5)\left(s^2+s+30\right)}{s^2(s+6)(s+5)}, \cdots \right.
$$
$$
\left. \frac{107.5(s+0.43)}{s}, \frac{400}{s} \right]
\tag{19}
$$

Calculation of the RGA matrix of system (17) evaluated at $s = 0$ yields

$$
\mathbf{\Lambda}\big(\mathbf{G}_{SVC}(s)\big) = \begin{bmatrix} 3.43 & -1.88 & -0.55 \\ -2.82 & 5.31 & -1.48 \\ 0.38 & -2.42 & 3.04 \end{bmatrix},
\tag{20}
$$

from where it can be seen that the selected input-output pairings are adequate (according to rule i in Section 1). It can be concluded that the compensator has no effect on the steady state coupling.

The input-output paring can be also investigated using the MSF. In addition, within the ICAD framework it is usual to evaluate the *structural robustness* by measuring the closeness of the Nyquist plot of the MSF to the complex point $(1, 0)$. In short, this allows measuring the robustness of the individual channels to become minimum-phase due to a controller $\mathbf{K}(s)$. A general discussion on this regard can be found in [Leithead and O'Reilly, 1992].

In order to measure *structural robustness*, the Bode plots of the negative of the MSFs are used (*i.e.*, $-\gamma_{ii}(s)$, $i = 1, 2, 3$), which allows classical robustness margins to be considered. These plots are shown in Figure 5, with a perfect control of the remaining variables being assumed. The input-output pairing should be made so that the diagonal MSFs, $\gamma_{ii}(s)$, have the lowest possible gain. Recall that a low coupling at frequency ω_0 is defined as $||\gamma_{ii}(j\omega_0)|| \approx 0$.
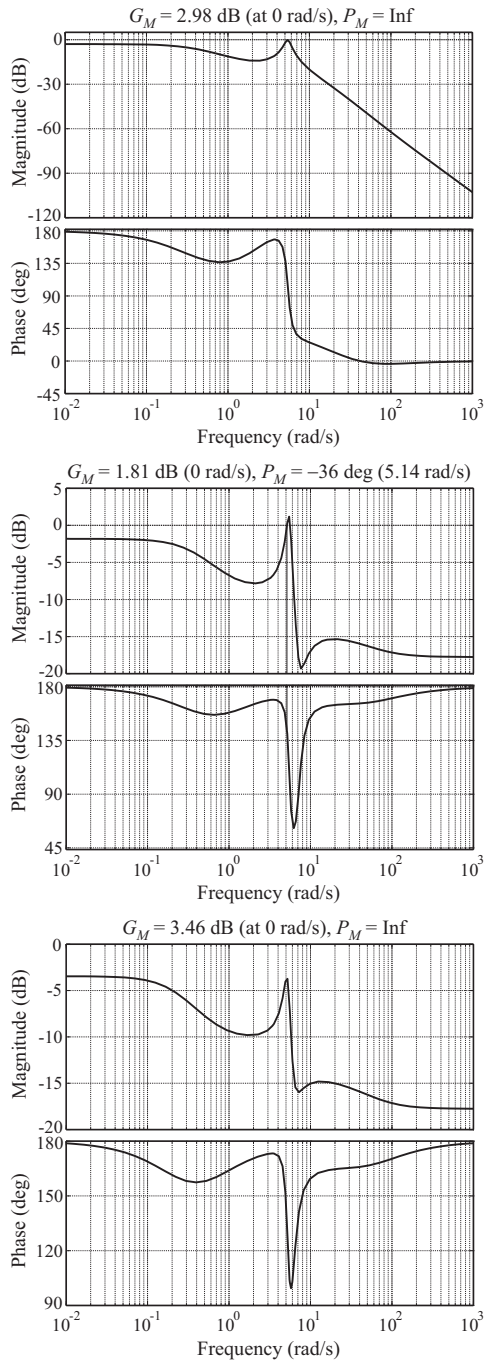
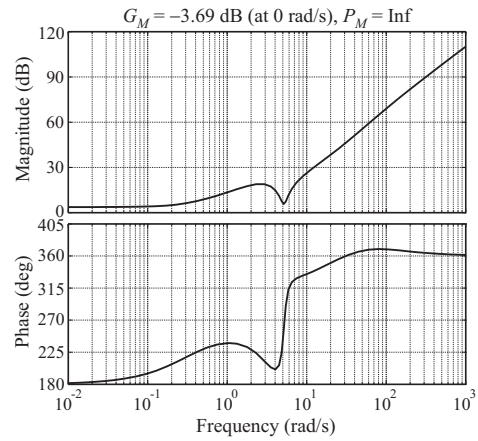Figure 5. Bode diagrams of $-\gamma_{ii}(s)$ $(i = 1, 2, 3)$.

Figure 6. Bode diagram of $-\gamma_{12}(s)$.

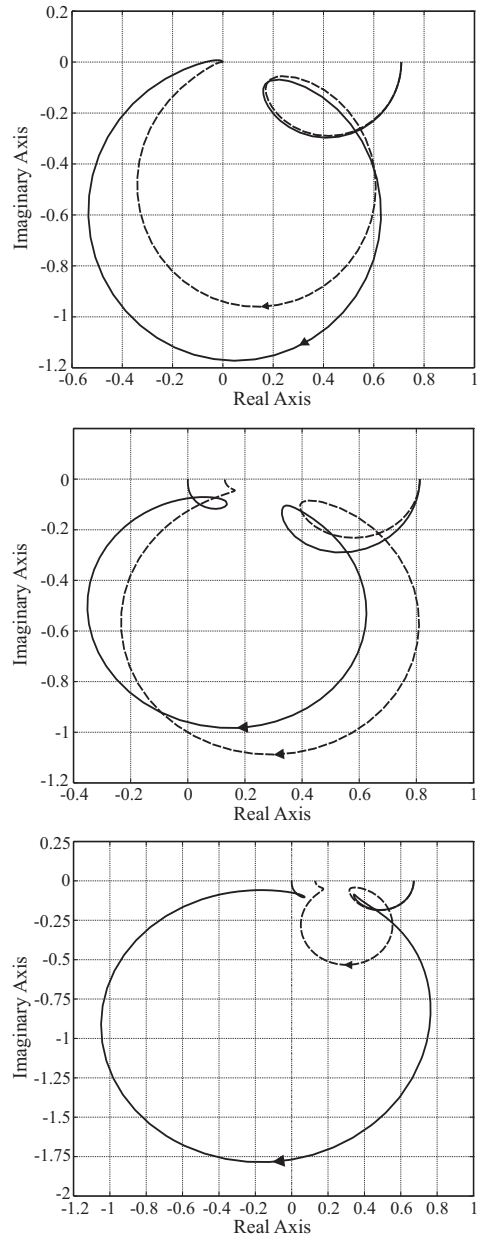

Figure 7. Nyquist plots of open loop (dotted line) and closed loop (continuous) MSFs of $\gamma_{ii}(s)$ $(i = 1, 2, 3)$.

For comparison, consider the Bode diagram of $-\gamma_{12}(s)$, which would result if input 1 was paired with output 2. This is shown in Figure 6. The plot suggests that paring input 1 with output 2 results in Individual Channel 1 being highly coupled with Multi-channel 2-3; thus, this configuration is not recommended. Further examination of the open loop MSFs is omitted in this paper due to space limitations. However, the results are in line with the RGA matrix (20).

Figure 5 shows that although the best input-output pairing selection has been already made, the system lacks structural robustness at low frequencies due to the closeness of the Bode plot to the critical phase and gain values (*i.e.*, 180° and 0 dB), especially in $\gamma_{11}(s)$.

This is where the MSF has advantages over the RGA matrix analysis. For a system to have adequate closed loop robustness the controller must not change the general shape of the Nyquist plot of the diagonal MSFs of the open loop system. The reason is that if the number of encirclements to the point $(1, 0)$ in the Nyquist plot of the MSF changes due to the controller, then the individual channels-zero structure in turn changes and additional non-minimum phase zeros may be induced. In order to assess this fact, the Nyquist plots of the open loop MSFs $\gamma_{ii}(s)$ (with $i = 1, 2, 3$) are shown in Figure 7. The Nyquist diagrams of the corresponding MSFs considering the effects of controller (19) are also shown (these MSFs can be calculated according to equation (10)).

Clearly the effect of controller (19) on the MSFs does not affect the structural robustness (closeness to the point $(1, 0)$). However, the coupling of individual channel 3 with Multi-channel 1-2 has increased. The interpretation of this result must be done carefully, as it does not mean that the closed loop will have increased cross-coupling. Actually, this means that by controlling $y_1(s)$ and $y_2(s)$ through $k_1(s)$ and $k_2(s)$, the remaining open loop system (i.e., output $y_3(s)$ with input $u_3(s)$) will now be more coupled. However, this coupling can be managed through $k_3(s)$ using the full individual channel transfer function (i.e., considering $k_1(s)$ and $k_2(s)$). On the other hand, the similarity of $\gamma_{11}(s)$ and $\gamma_{22}(s)$ with and without considering the actual controllers allows designing $k_1(s)$ and $k_2(s)$ almost as SISO systems considering the corresponding $\mathbf{H}(s)$ system as an identity (i.e., perfect control on the other variables). This clear assessment of robustness and coupling *during* the controller design process cannot be made with the RGA matrix alone.

6 Conclusion

The results presented in this paper fall short to fully appreciate the use of the ICAD framework. However, the analysis sheds light into the relationship between the MSF and the RGA matrix and allows visualizing how the MSF covers aspects that fall beyond the RGA matrix analysis. This is particularly clear in the control system design process. The MSF can be effectively considered an extended version of the RGA matrix which allows to consider the effect of specific controllers to the robustness of the system and assess the cross-coupling between groups of input-output pairs – among other applications.

References

Aree, P. and Acha, E. (1999). Block Diagram Model for Fundamental Studies of a Synchronous Generator-Static VAr Compensator System. *IEE Proceedings - Generation, Transmission & Distribution*, **146**(5), pp. 507–514.

Bristol, E. (1966). On a new measure of interaction for multivariable process control. *IEEE Transactions on Automatic Control*, **11**(1), pp. 133–134.

Chiu, M. S. and Arkun, Y. (1990). Decentralized control structure selection based on integrity considerations. *Industrial & Eng. Chemistry Research*, **29**(3), pp. 369–373.

Cook, M. V. (2012). *Flight Dynamics Principles: A Linear Systems Approach to Aircraft Stability and Control.* Butterworth-Heinemann, USA.

Grosdidier, P., Morari, M. and Holt, B. R. (1985). Closed-loop properties from steady-state gain information. *Industrial & Eng. Chemistry Fundamentals*, **24**(2), pp. 221–235.

Helton, J. W., Stankus, M. and Wavrik, J. J. (1998). Computer simplification of formulas in linear systems theory. *IEEE Transactions on Automatic Control*, **43**(3), pp. 302–314.

Leithead, W. E. and O'Reilly, J. (1992). M-Input m-output Feedback Control by Individual Channel Design. Part 1. Structural Issues. *International Journal of Control*, **56**(6), pp. 1347–1397.

Licéaga-Castro, E., Licéaga-Castro, J. and Ugalde-Loo, C. E. (2005). Beyond the Existence of Diagonal Controllers: from the Relative Gain Array to the Multivariable Structure Function. In *44th IEEE Conference on Decision and Control, and European Control Conference (CDC-ECC)*, Sevilla, Spain, Dec. 12-15, pp. 7150–7156.

Licéaga-Castro, E., Licéaga-Castro, J., Ugalde-Loo, C. E. and Navarro-López, E. M. (2008). Efficient multivariable submarine depth-control system design. *Ocean Engineering*, **35**(17–18), pp. 1747–1758.

Licéaga-Castro, J., Amézquita-Brooks, L. and Licéaga-Castro, E. (2008). Induction motor current controller for Field Oriented Control using Individual Channel Design. In *IEEE 34th Annual Conference of Industrial Electronics (IECON)*, Orlando, USA, Nov. 10-13, pp. 235–240.

Licéaga-Castro, J., Licéaga-Castro, E. and Amézquita-Brooks, L. (2005). Multivariable gyroscope control by individual channel design. In *IEEE Conference on Control Applications (CCA)*, Canada, Aug. 28-31, pp. 785–790.

Licéaga-Castro, J., Ramírez-España, C. and Licéaga-Castro, E. (2006). GPC control design for a temperature and humidity prototype using ICD analysis. In *Computer Aided Control System Design (CACSD), IEEE International Conference on Control Applications (CCA), IEEE International Symposium on Intelligent Control*, Oct. 4-6, pp. 978–983.

Mc Avoy, T., Arkun, Y., Chen, R., Robinson, D. and Schnelle, P. D. (2003). A new approach to defining a dynamic relative gain. *Control Engineering Practice*, **11**(8), pp. 907–914.

Mithulananthan, N., Canizares, C. A., Reeve, J. and Rogers, G. J. (2003). Comparison of PSS, SVC, and STATCOM controllers for damping power system oscillations. *IEEE Transactions on Power Systems*, **18**(2), pp. 786–792.

O'Reilly, J. and Leithead, W. E. (1991). Multivariable control by 'individual channel design'. *International Journal of Control*, **54**(1), pp. 1–46.

Skogestad, S. and Postlethwaite, I. (2005). *Multivariable Feedback Control*. John Wiley & Sons, UK.

Ugalde-Loo, C. E. (2009). *Dynamical modelling of power systems with power electronic controllers using individual channel analysis and design*. PhD dissertation, The University of Glasgow.

Ugalde-Loo, C. E., Acha, E. and Licéaga-Castro, E. (2010). Fundamental Analysis of the Electromechanical Oscillation Damping Control Loop of the Static VAr Compensator using Individual Channel Analysis and Design. *IEEE Transactions on Power Delivery*, **25**(4), pp. 3053–3069.

Ugalde-Loo, C. E., Acha, E., Licéaga-Castro, E. and Licéaga-Castro, J. U. (2008). Fundamental Analysis of the Static VAr Compensator Performance using Individual Channel Analysis and Design. *International Journal of Emerging Electric Power Systems*, **9**(2), pp. 1–35.